A pan-cancer analysis of RGR opsin expression and its downregulation associated with poor prognosis in glioma

Jianglong FENG[1,2,3,#], Wei ZHANG[2,#], Wen ZENG[2,#], Yu WANG[2], Yangguang GU[2], Yinghua LAN[2], Wenxiu YANG[3], Hongguang LU[1,2,*]

[1]School of Public Health, Guizhou Medical University, Guiyang, Guizhou, China; [2]Department of Dermatology, Affiliated Hospital of Guizhou Medical University, Guiyang, Guizhou, China; [3]Department of Pathology, Affiliated Hospital of Guizhou Medical University, Guiyang, Guizhou, China

*Correspondence: hongguanglu@hotmail.com
#Contributed equally to this work.

Retinal G protein-coupled receptor (RGR) serves a retinal photoisomerase function to mediate retinoid metabolism and visual chromophore regeneration in the human eyes. Retinoids display critical functions in cell proliferation, differentiation, and apoptosis. Abnormal retinoid metabolism may contribute to tumor development. However, in human tumor tissues, the expression of RGR remains uncharacterized. Herein, we performed the analysis of RGR expression in 620 samples from 24 types of tumors by immunohistochemistry (IHC) and 33 cancer types from the Cancer Genome Atlas (TCGA), the Chinese Glioma Genome Atlas (CGGA), and Gene Expression Omnibus (GEO) databases by bioinformatic analyses. Furthermore, the biological role of RGR in glioma cells was investigated using molecular biology approaches *in vitro*. Notably, we found that brain lower grade glioma (LGG), in contrast to other tumor types, had the highest median score of IHC and RNA level of RGR expression. Survival analysis showed that low RGR expression was associated with worse overall survival in LGG (p<0.0001). RGR expression levels in glioma were also associated with pathological subtypes, grades, and isocitrate dehydrogenase (IDH) mutations. Moreover, its molecular function was closely associated with cadherin-related family member 1 (CDHR1), a tumor-suppressive protein in glioma, suggesting that RGR might negatively regulate the tumorigenesis and progression of LGG through interacting with CDHR1. Our findings provide new insight into the role of RGR in human cancer, especially in glioma.

Key words: RGR; pan-cancer; glioma; CDHR1; overall survival

Retinal G protein-coupled receptor (RGR), as a member of the non-visual opsin subfamily expresses in Müller glia and the retinal pigment epithelium (RPE) in human eyes [1, 2]. To restore light sensitivity in the visual process, visual opsins need recharging with 11-cis-retinal (chromophore) [2]. Upon daylight condition, RGR in the RPE and Müller cells is capable of photoisomerizing all-trans-retinaldehyde to 11-cis-retinaldehyde, which continuously supplies the chromophore to visual opsins, explaining how the eye can retain responsiveness to daylight [3–5]. In addition, some studies have shown that RGR can also indirectly mediate the classical retinoid cycle that regenerates 11-cis-retinal independent of light, by enhancing the key enzyme of RPE-specific 65 kDa (RPE65) activity [6, 7]. Other studies revealed that RGR in RPE65-deficient mice still regenerates 11-cis-retinal in photic conditions, whereas the double knockout of RGR and RPE65 mice lost the sensitivity to light stimulation in the eye [8, 9]. Moreover, both previous sequence analysis and site-directed variant studies found that the conserved lysine residue at position 255 is critical for the Schiff base formation at bovine RGR, which is identified as the retinal-binding site in visual pigments [5, 10]. Given that RGR shares high homology with retinochrome, in which glutamic acid 161 serves as the counterion in retinochrome, the glutamic acid 156 in the transmembrane helices VI and V of RGR could act as the counterion to stabilize the retinal [10, 11]. Thus, these findings identified the structure basis of RGR covalent binding to retinal. Collectively, previous findings suggest that RGR serves a retinal photo-isomerase function to mediate retinoid metabolism in the human eyes. Since retinoids display critical functions in cell proliferation, differentiation, apoptosis, and aberrant retinoid signaling are

associated with human carcinogenesis [12, 13], it is intriguing to speculate that RGR may be associated with the initiation and development of cancers.

In the human genome, the RGR is composed of seven exons on chromosome 10q23 [14, 15]. Previous studies reported that the point variant of p.Ser66Arg and frameshift mutations that occurred in the human RGR are associated with retinal dystrophies and age-related macular degeneration [16–19]. Interestingly, both the RGR Ser66Arg mutation and a cis-acting mutation of cadherin-related family member 1 (CDHR1) in its nearby gene have been previously described in some patients with retinal dystrophies [17, 20]. Therefore, these evidences suggest that RGR is a necessary element in the visual sense, and its function is potentially related to the nearby gene of CDHR1. A recent study showed that downregulated CDHR1 is a poor prognostic factor in glioma patients while its overexpression can inhibit tumor cell proliferation and invasion [21]. Moreover, we found that RGR has higher expression in the proliferative lesions of psoriasis, seborrheic keratosis, and squamous cell carcinoma compared with normal skin tissues by immunohistochemistry (IHC) staining [22]. These interesting findings indicate that RGR might be related to the initiation and development of cancers. However, the functions of RGR in extraocular tissues such as the brain or skin remain almost completely unknown.

Here, we focused on the expression and characterization of RGR in different human cancers, as well as its association with clinical prognosis. We firstly performed the expression of RGR in 24 types of cancers via IHC staining, and further its gene expression level and survival analysis were evaluated among 33 tumor types by The Cancer Genome Atlas (TCGA) data. As a result, compared with other cancers types, there was significant difference between overall survival (OS) and different RGR expression level in brain lower grade glioma (LGG). Thus, LGG was selected first as a candidate to further study the correlation between RGR and the pathological subtypes, grades, and isocitrate dehydrogenase (IDH) mutation. Lastly, the biological function of RGR was studied by bioinformatics and cell biology experiments.

Patients and methods

Data collection. Our cohort was composed of 24 types of tumors, from the Affiliated Hospital of Guizhou Medical University. Hematoxylin and eosin (H&E) stained sections were reviewed and evaluated, and samples fulfilling the criteria for the appropriate diagnoses of various cancers were selected for study. Archived formalin-fixed paraffin-embedded (FFPE) blocks were cut to make 4 μm sections for IHC and multiple immunofluorescence staining. The gene expression data and related clinical overall survival information for 33 tumor types were collected from TCGA datasets (https://portal.gdc.cancer.gov/), while the gene expression

data for glioma was obtained from the Chinese Glioma Genome Atlas (CGGA) dataset (http://www.cgga.org.cn/index.jsp). In addition, the Gene Expression Omnibus (GEO) databases (https://www.ncbi.nlm.nih.gov/geo/) of glioma, including GSE21354, GSE16011, GSE107850, and GSE30472, were used to validate the expression and characterization of RGR in glioma. The pan-cancer analysis of RGR mutations was assessed by the cBio Cancer Genomics Portal tool (http://cbioportal.org) [23].

Ethics approval and consent to participate. The study was approved by the Ethics Committees of Affiliated Hospital of Guizhou Medical University; Approval: #2019-184 and was performed according to the Declaration of Helsinki. Under Chinese law, written consent from the patients was not required because the material used had been collected for diagnostic and therapeutic purposes in the archives of the Institute for Pathology, Affiliated Hospital of Guizhou Medical University, and used for this study in pseudonymized form.

RGR gene expression and survival analysis. RGR gene expression in the 33 kinds of cancers from TCGA data was analyzed using the Gene Expression Profiling Interactive Analysis (GEPIA) browser (http://gepia.cancer-pku.cn/) [24]. And, Kaplan-Meier (KM) survival curves combined with a log-rank test were used to test the differences in prognosis between high- and low-expressed RGR groups (according to the median expression value of RGR) using the survival R package [25]. RGR gene different expression and overall survival analyses in the glioma from CGGA and GEO datasets were analyzed using the Kaplan-Meier plotter online tools of CGGA (http://www.cgga.org.cn/analyse/RNA-data.jsp) and LOGpc (Long-term Outcome and Gene Expression Profiling Database of pan-cancers, http://bioinfo.henu.edu.cn/DatabaseList.jsp) [26], respectively.

Gene set enrichment analysis. Gene Ontology Molecular Function (GO_MF) and Kyoto Encyclopedia of Genes and Genomes (KEGG) analyses from TCGA LGG data were conducted using the LinkedOmics database platform (http://www.linkedomics.org/login.php) [27]. GO terms and KEGG pathways with p<0.05, False Discovery Rate (FDR) <0.25 were considered remarkably enriched.

IHC analyses of RGR expression. Details about the methods and further the semiquantitative assessment followed the previous report [28]. Briefly, 4 μm sections with different types of tumor tissues were dewaxed and rehydrated according to standard methods. Antigen retrieval was conducted with retrieval solution (ethylenediaminetetraacetic acid [EDTA], pH 9.0, ZLI-9069 from ZSGB-BIO, Beijing, China) for 4 min using the pressure cooker. The 3% H_2O_2 (PV-9000; ZSGB-BIO) was applied to block endogenous enzyme activity, subsequently incubated in a serum-free blocking solution (ZLI-9056; ZSGB-BIO). Then, the primary antibody of RGR (Affinity Biosciences, Cat# DF2858, RRID:AB_2840064) with dilution 1:300 was incubated at 4 °C overnight, followed by treatment with the

UltraView Polymer DAB Detection Kit (Ventana/Roche) according to the recommended manufacturing protocol.

RGR expression of all stained slides was scored by two independent investigators. The semi-quantitative assessment method was carried out by using percentages of 3+ (strong), 2+ (moderate), 1+ (weak), and 0 (negative) staining of tumor cells for each sample. The IHC score was calculated by the percentage of positive tumor cells ($3 \times$ x% $+ 2 \times$ x% $+ 1 \times$ x% $=$ total score) to equal a range of 0–300 [29].

Multiple immunofluorescence staining. Based on the previous method [30], co-staining of RGR and glial fibrillary acidic protein (GFAP; GeneTex, Irvine, CA, USA) in glioma tissues was performed. The steps from paraffin dewaxing and hydration to primary antibody incubation were the same as the above IHC staining method. After the first primary antibody of anti-RGR (1:300; Affinity Biosciences, Cat# DF2858, RRID: AB_2840064) overnight at 4 °C, the secondary antibody marked with HRP (abs50012; Absin, China) was incubated at room temperature (RT) for 30 min in the dark condition. Next, the sections were stained with monochromatic fluorescent dyes 570-tyramide signal amplification (TSA) solution (abs50012; Absin) at a 1:200 dilution for 30 min at RT in the dark. After repeating the above steps, the slides were again immersed in antigen and then stained with the second primary antibody of anti-GFAP (rabbit 1:100; GeneTex), corresponding secondary antibody, and monochromatic fluorescent dyes 520-TSA (abs50012; Absin), respectively. DAPI (abs50012; Absin) with 1:100 dilution at RT for 5 min was used for nuclei staining. According to the above steps, co-staining of RGR (1:300) and CDHR1 (PAS-43510, 1:100, Invitrogen, USA) in the glioma tissues was also conducted.

Image analysis of tissue cytometry was conducted by The TissueFAXS Quantitative Imaging System (TissueGnostics, Vienna, Austria) [31, 32]. The staining intensity of GFAP and RGR was quantitated by the computed mean grey level intensity in the cancer cell. The flow cytometry-like dot scatterplots were used to display the biomarker-positive cells in the immunofluorescence images.

Cell culture and transient transfection. U87 cell line was cultured in DMEM medium (Gibco, USA) containing 10% fetal bovine serum (FBS; SORFA, Beijing, China), 2 mM L-glutamine (Gibco, USA), and 1% (vol/vol) penicillin/streptomycin (Biological Industries, Kibbutz Beit Haemek, Israel) incubated at 37 °C in a 5% CO_2 incubator. Approximately 24 h after seeding into 96-well plates at 0.8×10^4 cells/well, in accordance with the manufacturer's instructions, cells were transiently transfected by Lipofectamine 2000 (2097561, Invitrogen, USA) with a final siRNA concentration of 40 nM. Transfection reactions were performed in serum-free Opti-MEM (31985070, Gibco). After siRNA transfection, cells were cultured for 48 h for further detection. Levels of RGR protein silencing were assessed 48 h post-transfection by western blotting. The pooled siRNA oligos targeting RGR (5'-AUGCCAUCCUGUAUCU-AUAUU-3'), and negative control siRNAs (5'-UAUAGAUA-CAGGAUGGCAUUT-3') were purchased from Tran Sheep Bio-Tech Co. Ltd. (Shanghai, China).

Western blot. Based on the previous method [33] briefly, the proteins (20 μg) of U87 cells were separated via 10% SDS-PAGE (Beijing Solarbio Science & Technology Co., Ltd., Beijing, China) for 1.5 h at 80 V and then were transferred onto polyvinylidene fluoride membranes (EMD Millipore, Billerica, MA, USA) for 90 min at 250 mA. Following blocking with 5% skimmed milk for 2 h at RT, the membranes were then incubated with primary antibody, including anti-RGR (cat. no. DF2858, 1:1000, Affinity Biosciences), anti-CDHR1 (PAS-43510, 1:1000, Invitrogen, USA) and a mouse anti-human beta-tubulin monoclonal antibody (cat. no. T0023; 1: 10000; Affinity Biosciences) overnight at 4 °C, respectively. Subsequently, the membranes were incubated with horseradish peroxidase (HRP)-labeled goat anti-rabbit (cat. no. ab6721; 1:10000; Abcam) or anti-mouse (cat. no. ab6789; 1:10000; Abcam) secondary antibodies for 60 min at RT. Finally, the membranes were visualized using a BeyoECL Plus kit (P0018S, Beyotime Institute of Biotechnology, Shanghai, China) with the Bio Imaging system (Bio-Rad Laboratories, Inc.).

CCK-8 assay. The cell proliferation was measured via Cell Counting Kit-8 (CCK-8) assay (Dojindo, Japan). In brief, the cells were seeded into a 96-well plate at a concentration of 1×10^4 cells with 10 μl CCK-8 per well. The cell growth rate at different time points (6 h, 12 h, 24 h, 48 h) was detected at 450 nm using a SkanIt Varioskan LUX microplate reader (Thermo Fisher Scientific).

Transwell invasion assay. Transwell invasion assays were conducted in the Transwell filter chamber with an 8 μm pore size (Corning, Lowell, MA, USA). U87 cells were suspended in a serum-free medium and added to the upper Transwell chamber at a density of 1×10^4 cells/200 μl medium. After 48 h of migration, the migrated cells were stained with 0.1% crystal violet (Solarbio, cat. G1063) for 15 min. Photographs were taken using an inverted microscope (Olympus, Japan). The number of cells from five random fields was counted using ImageJ software (imagej.nih.gov/ij).

Statistical analyses. R version 3.6.1 and GraphPad Prism (version 8.0) software were used for statistical analysis. Continuous variables were presented as mean ± SD or median with interquartile range (IQR) when the distribution was skewed. The analysis of variance to compare the means of two or more than two groups was performed by t-tests or one-way. Both Mann-Whitney (two groups) and the Kruskal-Wallis (more than two groups) tests were used to compare the nonparametric distributions. Survival analyses were conducted via the Kaplan-Meier method. The time ROC (v 0.4) of R packages was used for ROC curves analysis. Statistically significant differences were considered when $p < 0.05$ (*$p < 0.05$, **$p < 0.01$, ***$p < 0.001$).

Results

Pan-cancer analysis of RGR expression in various cancers. General characteristics of 620 samples of 24 cancer types are highlighted in Table 1. The median IHC staining scores of RGR differed significantly among different tumor types (Figure 1A). The median RGR score was the highest in LGG (Median [IQR]) (150.0 [80.00–235.0]), while lowest in the diffuse large B-cell lymphoma group (30.00 [20.00–50.00]) (Table 1). Also, we compared the differential expression of the RGR gene in 33 cancer types using TCGA data [24], which showed that the Transcripts Per Kilobase of exon model per Million mapped reads (TPM) value of RGR RNA level was higher in 10 types of cancers such as breast invasive carcinoma, colon adenocarcinoma, and head and neck squamous cell carcinoma, compared with adjacent normal tissues (Figure 1B), while downregulating in those cancers of bladder cancer, glioblastoma multiforme (GBM), kidney chromophobe, lung squamous cell carcinoma. RGR RNA level was highest in LGG compared with other types of cancer (Figure 1B). Next, the RGR gene alterations were analyzed in two different pan–cancer datasets (500 samples from GSE186344 and 249 samples from BioStudies (ID: S-EPMC6119118)) from the cBioPortal database [34–35]. We found that the frequencies of gene mutations, including splice mutation and missense mutations, were 0.9%

(Figure 1C) and mainly occurred in melanoma of unknown primary and esophageal adenocarcinoma (Figure 1D).
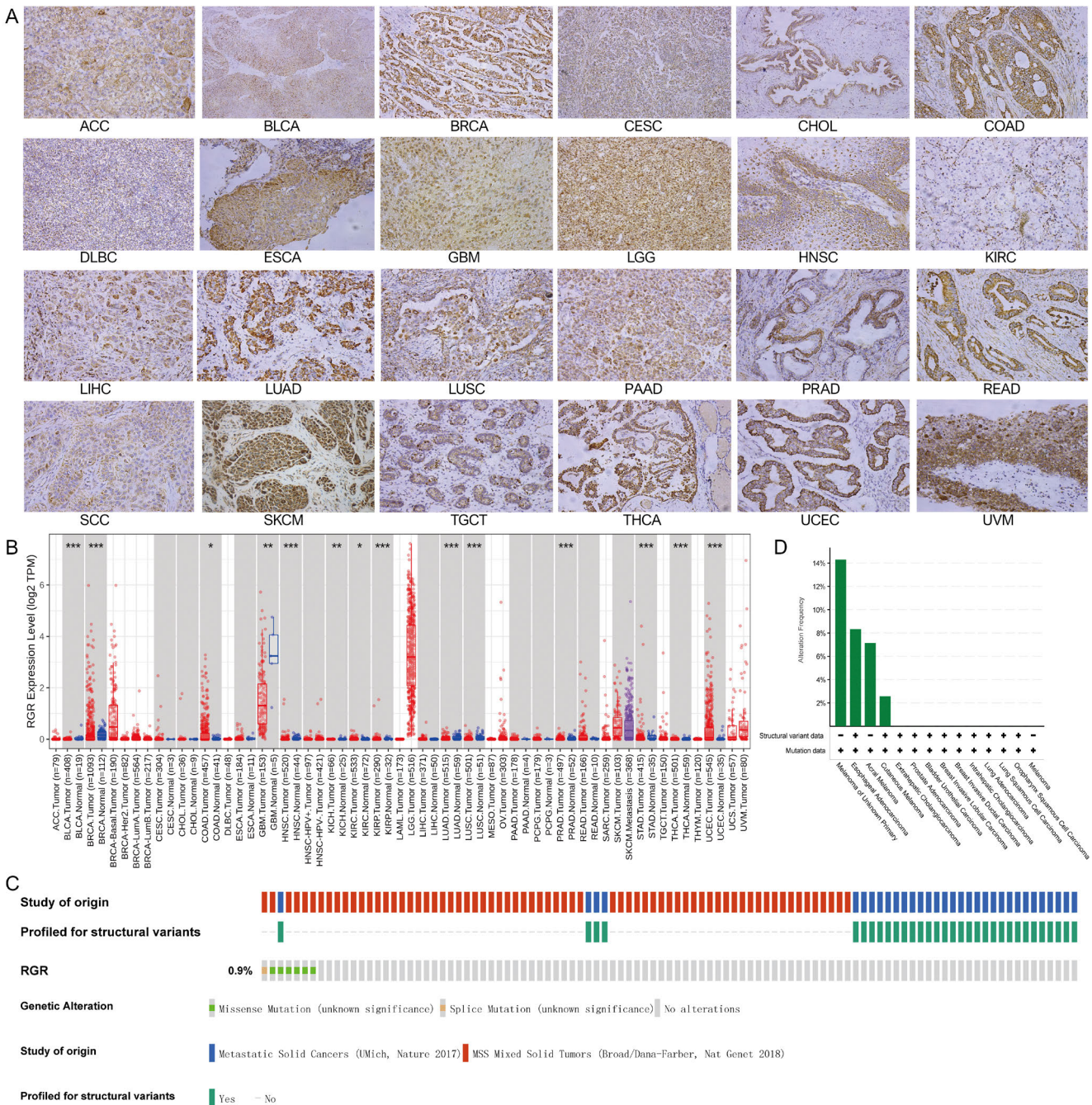
Survival analysis. Furthermore, using TCGA data, we estimated the associations between RGR expression level and survival status of the patients in 33 tumor types by log-rank tests. Only in LGG, the Kaplan-Meier survival analysis showed a significant difference (p<0.0001) of patient OS found between low and high expression of RGR groups according to RGR expression of median value (Supplementary Figures S1A, S1B), revealing that low RGR expression is associated with shorter OS. In addition, the effects of RGR on progression-free survival (PFS), disease-free survival (DFS), and disease-specific survival (DSS) were also tested in LGG. In TCGA datasets, we found that with the exception of DFS (p=0.656) (Supplementary Figure S2), RGR expression level affected the other two survival index of PFS (p<0.0001), DSS (p<0.0001) in LGG patients (Supplementary Figures S1C–S1F). Moreover, the associations between expression levels of RGR and glioma survival were evaluated using CGGA, GSE30472, and GSE107850 datasets. The results showed that in the CGGA dataset, patients with higher expression of RGR had longer OS than those with lower expression of RGR in grade III LGG and primary grade II LGG, while the difference was observed in recurrent GBM (Figure 2). Similar to the results from TCGA datasets, low expression of RGR in DFS analysis was a significantly poor prognosis among LGG

Table 1. RGR expression scores in 24 subtypes of cancers.

Tumor sites	Abbreviations	Tumor types	RGR expression IHC Score (median [IQR])
Adrenal cortex	ACC	Adrenocortical carcinoma (n=21)	40.00 [20.00–75.00]
Bladder	BLCA	Urothelial carcinoma (n=17)	110.0 [85.00–160.0]
Breast	BRCA	Carcinoma (n=20)	120.0 [85.00–187.5]
Cervix uteri	CESC	Squamous cell carcinoma (n=23)	75.00 [50.00–100.0]
Bile duct	CHOL	Cholangiocarcinoma (n=23)	120.0 [90.00–160.0]
Colon	COAD	Adenocarcinoma (n=28)	145.0 [120.0–180.0]
Blood	DLBC	Lymphoid neoplasm diffuse large B-cell lymphoma (n=27)	30.00 [20.00–50.00]
Esophagus	ESCA	Esophageal carcinoma (n=21)	100.0 [80.00–180.0]
Brain	GBM	Glioblastoma multiforme (n=32)	80.00 [60.00–120.0]
	LGG	Lower grade glioma (n=61)	150.0 [80.00–235.0]
Head/Neck	HNSC	Squamous cell carcinoma (n=21)	60.00 [40.00–90.00]
Kidney	KIRC	Clear cell carcinoma (n=28)	80.00 [62.50–100.0]
Liver	LIHC	Hepatocellular carcinoma (n=23)	40.00 [10.00–80.00]
Lung	LUAD	Adenocarcinoma (n=29)	100.0 [60.00–130.0]
	LUSC	Squamous cell carcinoma (n=26)	65.00 [47.50–80.00]
Pancreas	PAAD	Adenocarcinoma (n=22)	90.00 [60.00–145.0]
Prostate	PRAD	Adenocarcinoma (n=22)	95.00 [40.00–120.0]
Rectum	READ	Adenocarcinoma (n=26)	120.0 [90.00–165.0]
Skin	SCC	Squamous cell carcinoma (n=48)	120.0 [80.00–160.0]
	SKCM	Melanoma (n=38)	135.0 [80.00–212.5]
Testicular	TGCT	Testicular germ cell tumors (n=4)	90.00 [75.00–202.5]
Thyroid	THCA	Papillary carcinoma (n=22)	110.0 [80.00–165.0]
Endometrium	UCEC	Uterine corpus endometrial carcinoma (n=25)	90.00 [80.00–160.0]
Uvea	UVM	Melanoma (n=13)	120.0 [80.00–210.0]

patients from the GSE107850, however, there was no difference between RGR expression and prognosis of GBM in the GSE30472 dataset (Supplementary Figure S3). Also, in our LGG samples, based on the RGR score of median value, prognostic analysis was made between patients with high and low expression of RGR via the Kaplan-Meier method,

which showed low IHC score of RGR was associated with worse OS in LGG (p=0.023) (Supplementary Figure S4). Together, these results suggested that the downregulation of the RGR expression is associated with poor outcome of LGG. Following this, we focused on the expression characteristics and functions of RGR in LGG.

Figure 1. Expression difference of RGR in different tumor types. A) RGR expression in representative cancers cases from 24 tumor types via IHC staining (IHC, ×20 magnification). B) mRNA levels of RGR in 33 subtypes of cancers from TCGA. C) Mutation analysis of the RGR gene in two different pan-cancer datasets from the cBioPortal database (500 samples from GSE186344 and 249 samples from BioStudies (ID: S-EPMC6119118)). D) Tumor types of RGR variants in two different pan-cancer datasets (500 samples from GSE186344 and 249 samples from BioStudies (ID: S-EPMC6119118)).

Figure 2. Overall survival analysis of glioma patients between low and high expression of RGR groups in CGGA dataset according to RGR expression of median value using the Kaplan-Meier method.
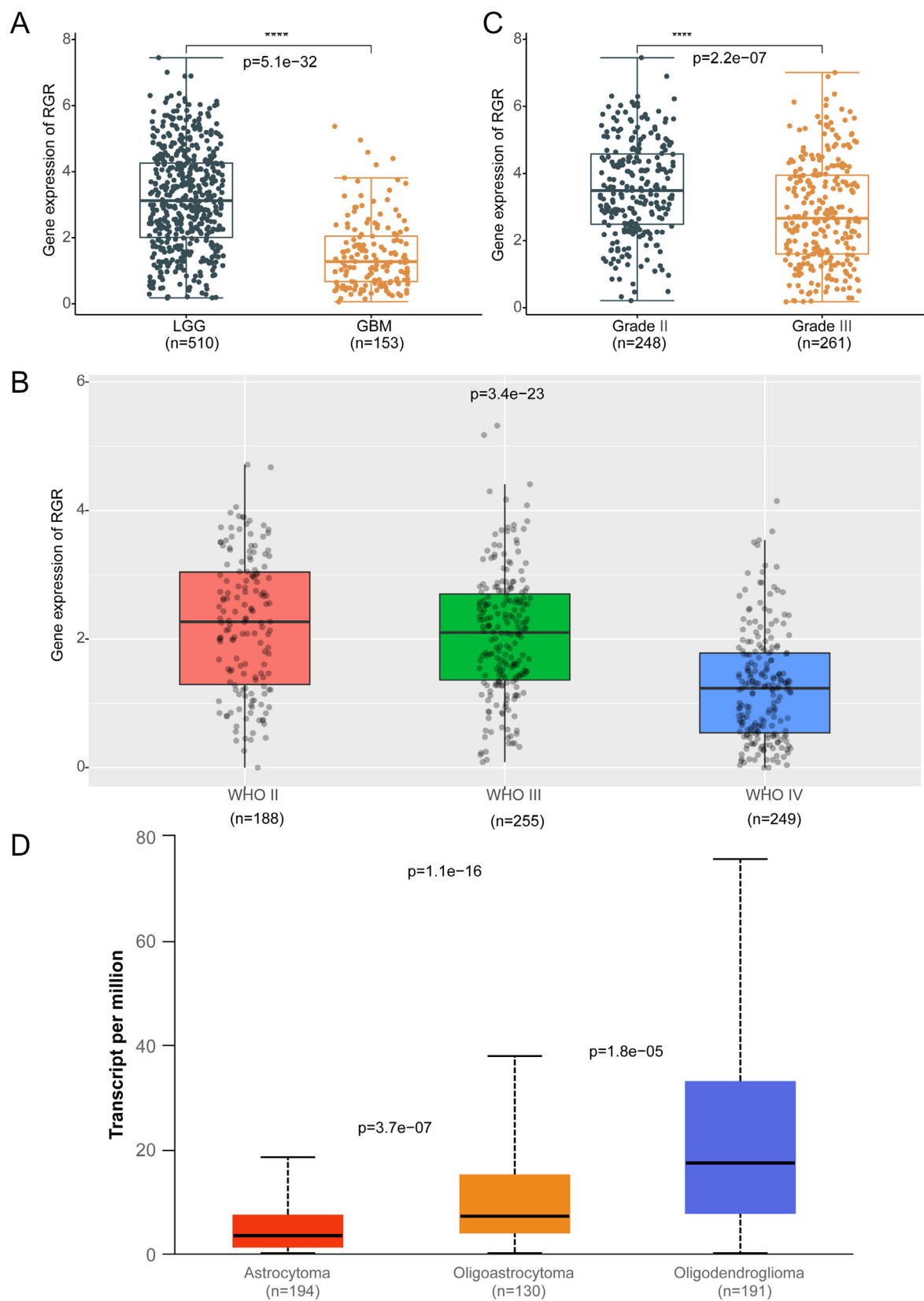
Figure 3. Gene expression of RGR in different pathological subtypes and grades of glioma in TCGA (A, C, D) and CGGA (B) datasets. ***p<0.001

Association between RGR and histopathologic variables of LGG. Considering LGG is grade II–III glioma with grade IV glioma also termed GBM, we first compared the gene expression difference of RGR between GBM and LGG in TCGA and CGGA datasets (Figure 3). In contrast to GBM, the RGR gene was expressed at a higher level in LGG (p<0.0001). Also, there was a notable difference in RGR expression between grade II and III LGG patients (p<0.0001), with a higher level of RGR in grade II LGG via TCGA data (Figures 3A–3C). Moreover, RGR gene expression in three cellular morphologic subtypes of LGG including astrocytoma, oligoastrocytoma, and oligodendroglioma were compared using TCGA data. The results showed that RGR was downregulated in astrocytoma compared with the other subtypes (Figure 3D). At the protein level, RGR also showed the same expression trends, and its expression decreased gradually from grade II to IV glioma through the multi-immunofluorescence staining and tissue cytometry analysis (Figure 4). In addition, there were no statistical significances between RGR expression level and clinicopathological data including age, sex, and progression status (Supplementary Figure S5). In other types of cancer, the association between RGR and histopathologic variables

was performed. RGR expression level was significantly correlated with the pathological stage of tumors involving adreno-cortical carcinoma, cholangiocarcinoma, kidney renal clear cell carcinoma, and stomach adenocarcinoma. We also found that the RGR expressions in different histological types of cancers were obviously different including bladder urothelial carcinoma, cervical squamous cell carcinoma, and endocervical adenocarcinoma. The expression of RGR in colon adenocarcinoma/rectum adenocarcinoma, head and neck squamous cell carcinoma, and liver hepatocellular carcinoma is significantly associated with lymphatic and/or vascular invasion (Supplementary Figure S6).

Expression of RGR in IDH mutant LGG and its correlation with CDHR1. Next, we assessed the relationships of RGR with IDH mutations in LGG. As shown in our LGG specimens, RGR expression was higher in the IDH1 R132H mutation group than IDH wild-type group in LGG patients (p=0.0325). Also, RGR expression in grade II–IV gliomas with IDH mutation 1p19q deletion or IDH mutation 1p19q non-deletion was higher in the CGGA dataset, compared with IDH wild-type gliomas (p<0.005) (Figure 5A). By comparison with IDH mutation 1p19q non-deletion, RGR
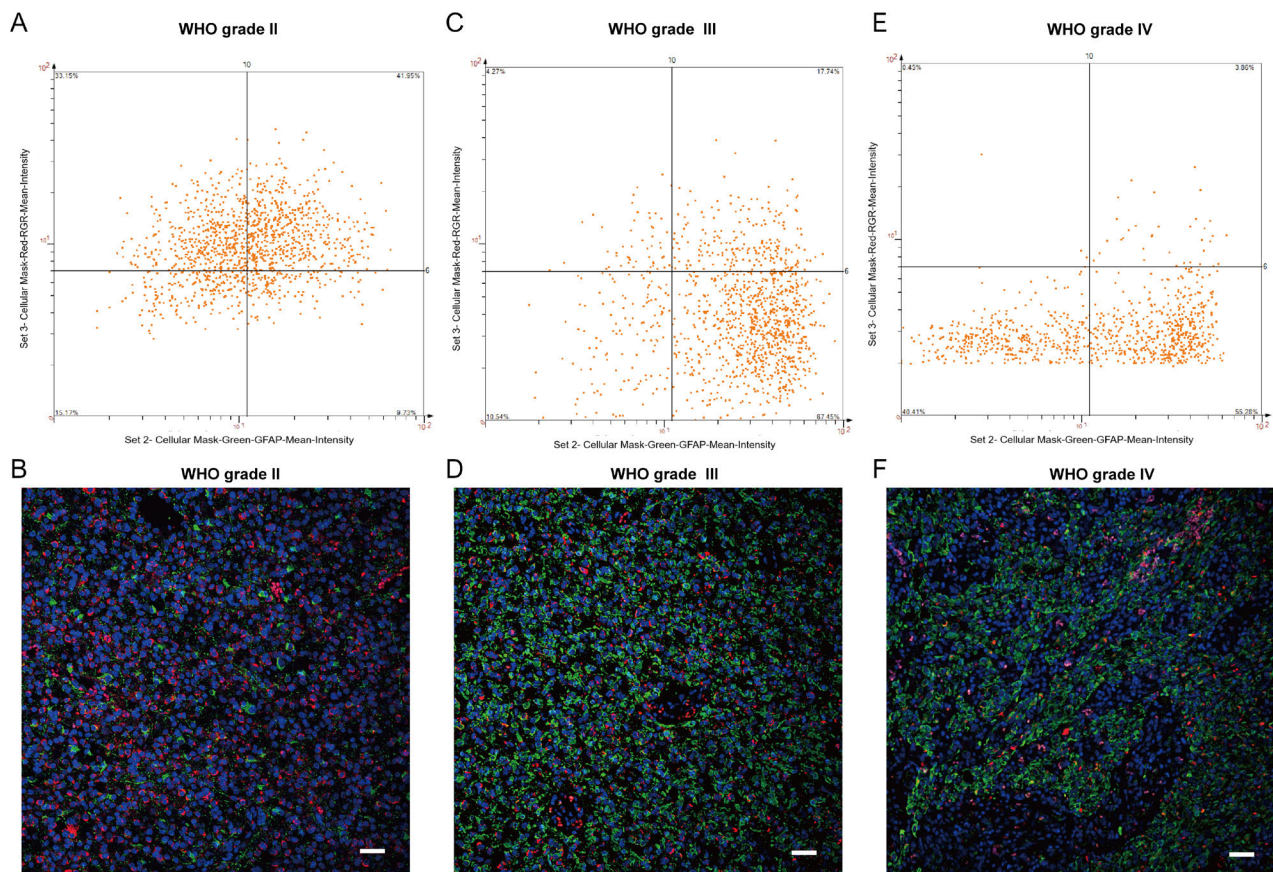

Figure 4. Scatterplot of RGR and GFAP expression on individual cells of glioma tissues using multiple immunofluorescence staining and tissue cytometry (A, C, E) assays. Multi-immunofluorescence analysis of representative case from gliomas (B, D, F). The cancer cells were positive by co-staining of GFAP (green) and RGR (red). Scale bars: 20 μm
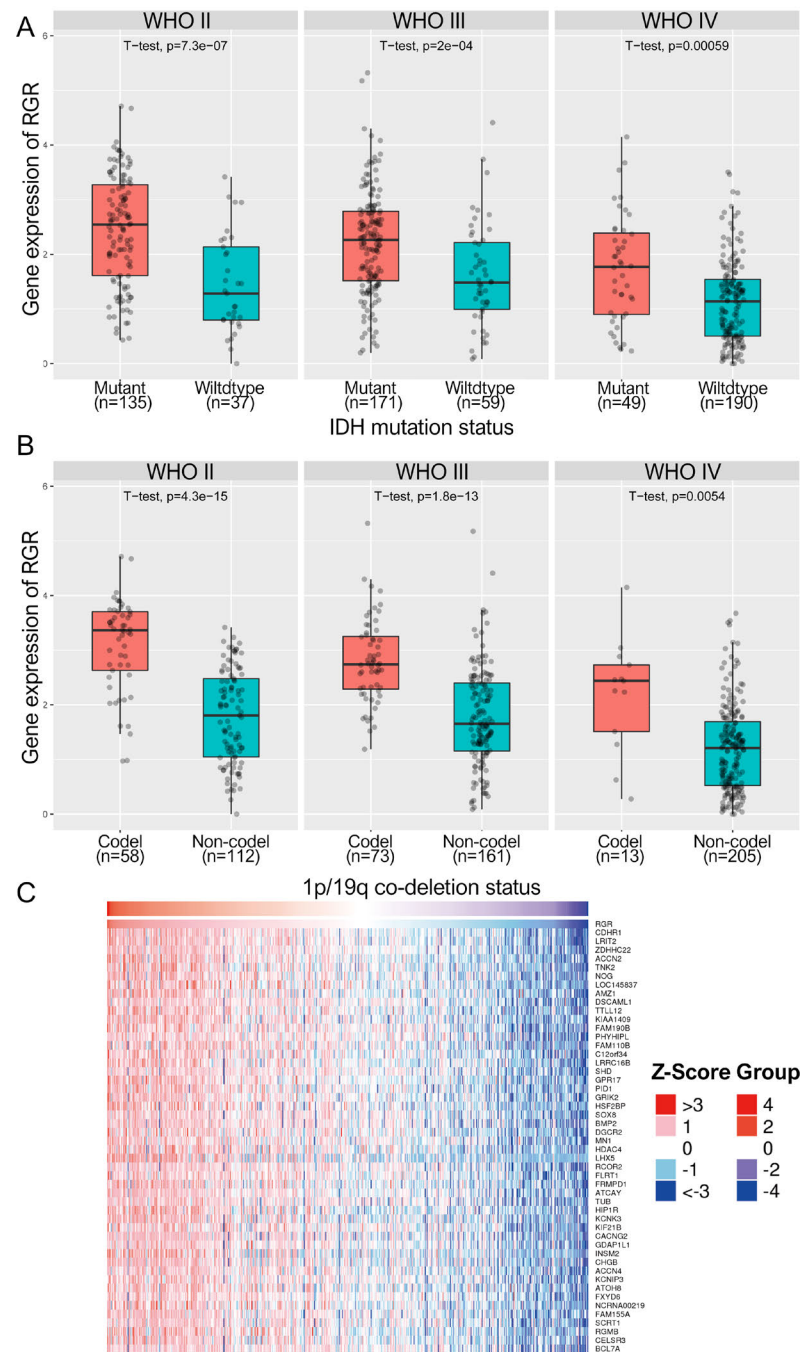
Figure 5. RGR expression levels in glioma associated with isocitrate dehydrogenase (IDH) mutations (A, B). The heat map of co-expressed genes of RGR in LGG (C). RGR was significantly and positively correlated with CDHR1 expression in TCGA dataset.

was also highly expressed in grade II–IV glioma patients with IDH mutation 1p19q deletion in the CGGA dataset (Figure 5B). We then measured TCGA mRNA-seq data by Pearson's correlation analysis between RGR and its co-expressed genes. And, the most relevant result showed a significantly positive correlation between RGR and CDHR1 expression in the heat map (r=0.75, p<0.0001) (Figure 5C), and the results of

their correlation analysis are consistent in GEO (Supplementary Figures S7A, S7B) and CGGA datasets (Supplementary Figure S7C). A recent study demonstrated that low expression of CDHR1 has been identified as a poor prognostic factor in LGG [21]. Thus, these promising findings indicated that RGR may be a potential indicator for the assessment of LGG prognosis.

Differential gene analysis of RGR in LGG. To further investigate the potential molecular mechanism of RGR in LGG, in TCGA cohort, we performed the differential gene analysis between samples with low and high RGR expression to identify RGR-related signaling pathways using GO and KEGG pathway enrichment analyses. As shown in Figure 6, the notably downregulated terms were primarily enriched in "cell adhesion molecule binding", "ECM-receptor interaction", "Cytokine receptor binding", "Cytokine receptor activity", "Extracellular matrix structural constituent", and "Cytokine-cytokine receptor interaction", partly involved in cell adhesion. Thus, these results may provide insights into the cellular biological effects of RGR that could regulate tumor cell adhesion by interacting with CDHR1 in LGG and further affect tumorigenesis and progression.

Effects of RGR downregulation on the proliferation and invasion of glioma cells. To determine if RGR mediates proliferation, migration, and invasion in glioma cells, we first

investigated the main location of RGR and CDHR1 in glioma tissues using a fluorescence microscope. We found that both RGR and CDHR1 were mainly distributed in the cytoplasm and membrane of cancer cells in LGG and GBM (Figure 7A), and their expression patterns are similar in cancer tissues. Next, we reduced RGR mRNA levels in the glioma cell line of U87 cells using small RNA interference technology. The protein level of CDHR1 was significantly reduced under RGR low expression in U87 cells (Figures 7B, 7C). Furthermore, the cell growth was tested via the CCK-8 assay, which was significantly promoted by the downregulated RGR in U87 cells (Figure 7D). Also, the cell invasion was enhanced under low expression of RGR in U87 cells as assessed by the Transwell assay (Figures 7E, 7F). Taken together, those results suggest that low-expressed RGR has notably impacted on the proliferation and invasion of glioma cells. Bases on the relationship between RGR and CDHR1, we speculated that RGR and CDHR1 may form a molecular complex. To study
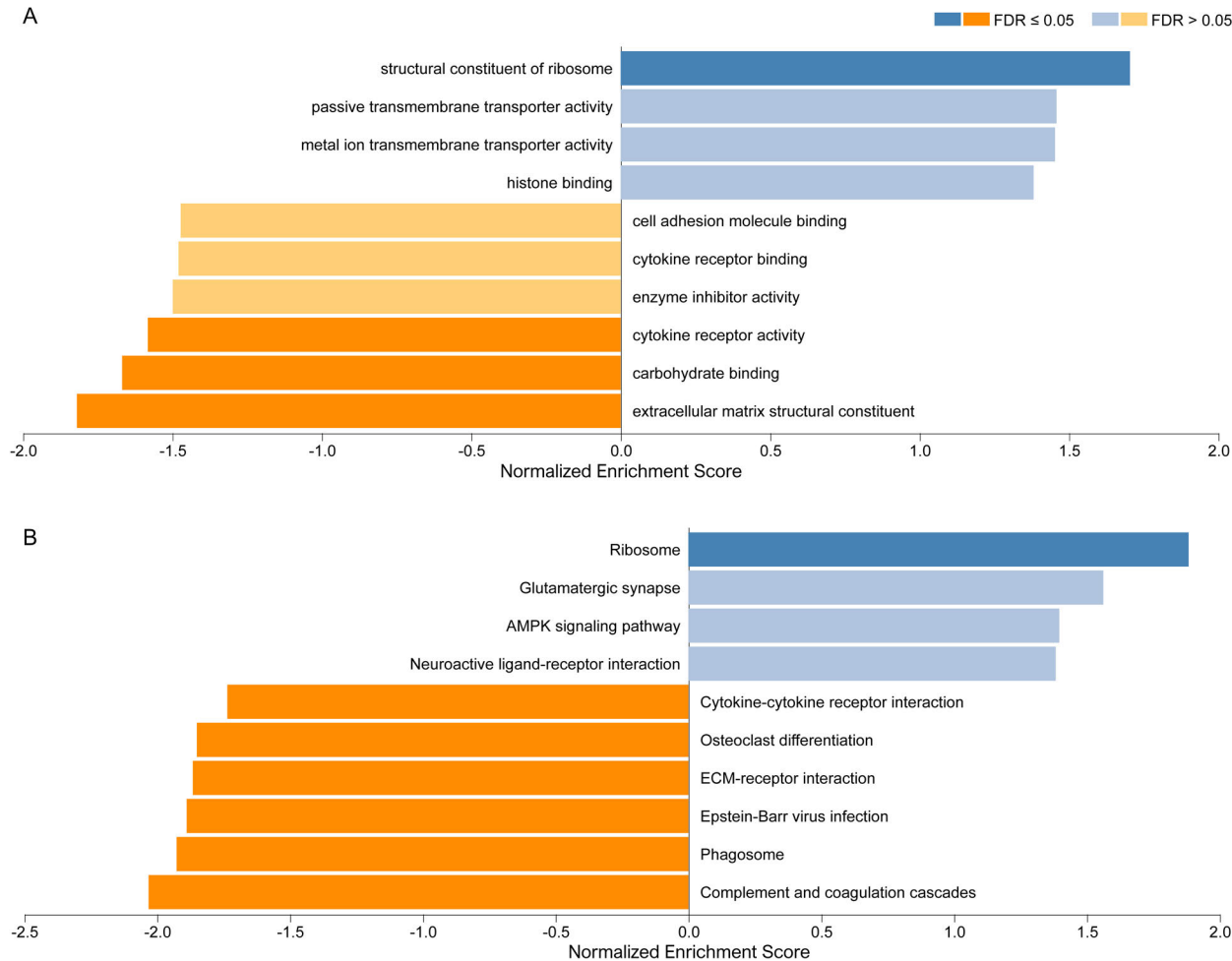

Figure 6. Gene set enrichment analysis of RGR. The GO (A) and KEGG (B) pathways that were enriched by the top-ranked genes in the two groups were detected by GSEA. For each analysis, the number of gene set permutations was set to 1000. The nominal (NOM) P value, false discovery rate (FDR <0.25), and normalized enrichment score (NES) were used to identify the pathways enriched in each phenotype.
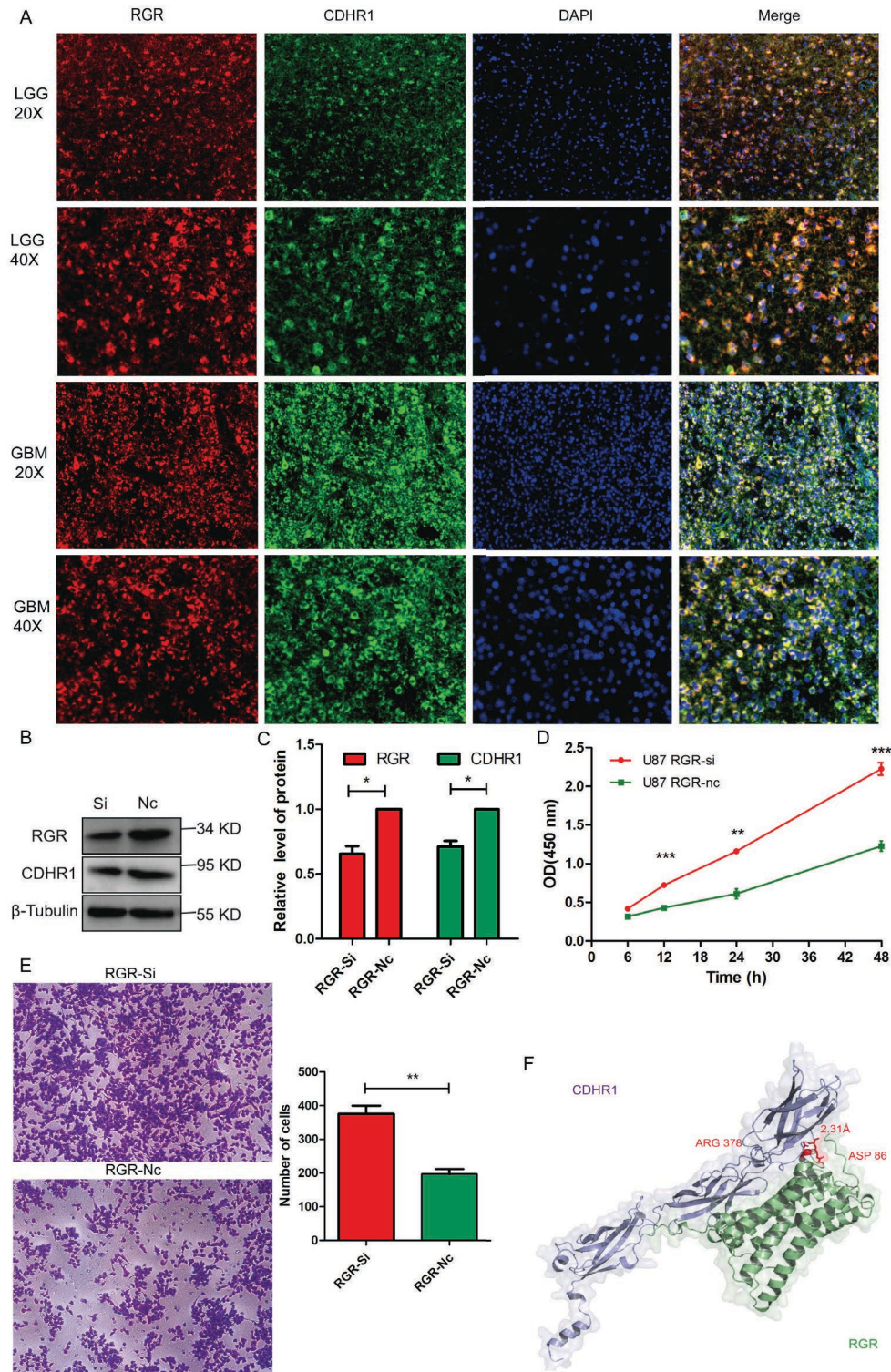
Figure 7. Low expression of RGR increase glioma cell growth and invasion. A) Cell localization of RGR and CDHR1 in LGG and GBM tissues using multiple-immunofluorescence staining (×20, ×40 magnification). **B)** The effect of RGR siRNA on the protein level of RGR and CDHR1 expression (Si: siRNA, Nc: negative control). **C)** The relative protein level was quantified using ImageJ software (RGR-Si *vs.* RGR-Nc: p=0.0044; CDHR1-Si vs. CDHR1-Nc: p=0.0022). **D)** Cell growth analysis of U87 under RGR low expression by CCK-8 method (12h: p=0.004; 24h: p=0.0014; 48h: p=0.007). **E)** Representative images of invasive U87 cells under RGR low expression using Transwell assay. **F)** The quantification of migrated U87 cells under RGR low expression using ImageJ software (p=0.0033). **G)** The interaction between RGR and CDHR1 was performed by molecular docking in glioma. *p<0.05, **p<0.01, ***p<0.001

the protein-protein interaction between RGR and CDHR1, we used the ZDOCK method for homology modeling to estimate the interaction between RGR and CDHR1 [36]. The results showed that the binding site of ASP86 in RGR interacted with the ARG378 residue of CDHR1 (Figure 7G), indicating that RGR and CDHR1 can form a physical complex to regulate the proliferation and invasion of glioma cells.

Discussion

Retinal G protein-coupled receptor (RGR) functions as a retinal photo-isomerase to mediate retinoid metabolism in the human eyes. Retinoids are a class of natural and/or synthetic vitamin A analogs including vitamin A, all-trans retinoic acid, and related signaling molecules that are involved in the physiology of vision and regulating the proliferation and differentiation of various types of normal and malignant cells [13]. Retinoid signaling is impaired early in the carcinogenesis of various cancers, such as cancers of the oral cavity, skin, bladder, kidney [13, 37–39]. Retinoids are also used to treat human cancers, in part due to their ability to inhibit cell proliferation, induce differentiation, and cell death by apoptosis [13]. Thus, those suggested that RGR may be associated with tumor development in various human cancers. However, the biological functions of RGR in extraocular tissues including tumors remain unclear. The expression and characterization of RGR in various tumors are also barely reported. Herein, in this study, we started with a pan-cancer analysis of RGR opsin expression using TCGA datasets in 33 cancer types, among which 14 were shown to be differentially expressed at the transcriptional levels of RGR compared with adjacent normal tissues. Moreover, we found that RGR expression level was significantly correlated with histological types, pathological stage, and/or lymphatic and/or vascular invasion of various types of human cancers. These results revealed that RGR expression is heterogeneous across multiple tumors, which suggested that abnormal expression of RGR may play a role in oncogenesis and tumor development of various human cancers. Particularly, we found that low expression of RGR in glioma tissue was remarkably associated with poor prognosis in glioma patients and other validated prognostic factors including histological grade, IDH mutation, and CDHR1 [21, 40, 41], suggesting that downregulation of RGR may contribute to carcinogenesis in glioma, especially in LGG. Altogether, our results implied that RGR may act as a tumor-negative gene in LGG carcinogenesis and progression.

To our knowledge, however, the molecular functions of RGR in cancer have not yet been reported. Therefore, we conducted bioinformatics analysis to study the molecular mechanisms of RGR in LGG carcinogenesis and progression via TCGA datasets. These results demonstrated that RGR in LGG remarkably correlates with "cell adhesion molecule binding" and "ECM-receptor interaction", which are related to cell adhesion. Thus, those indicated that RGR may affect the LGG carcinogenesis and progression by regulating cancer cell adhesion. Furthermore, a highly positive correlation was shown between RGR and the CDHR1 gene via Pearson correlation analysis. We also determined the biological functions of RGR and the expression relationship between RGR and CDHR1 in U87 glioma cells. A positive correlation was shown between RGR and CDHR1 expression, and low expression of RGR reduced the expression of CDHR1 protein level and enhanced the proliferation and invasion of glioma cells *in vitro*, which is consistent with our previous results of bioinformatics analysis. The CDHR1, also known as protocadherin 21 (PCDH21), is a photoreceptor-specific cadherin and belongs to the non-clustered PCDHs of cadherin superfamily, wherein loss of expression of some non-clustered PCDHs, such as PCDH1, PCDH10, and PCDH20, are associated with unfavorable prognosis of various human cancers [42–45], which indicated that most non-clustered PCDHs of calcium-dependent cell-cell adhesion molecules may exert tumor-suppressive function [43]. It is further supported by a recent report that downregulated CDHR1 is a poor prognostic factor in glioma patients while its overexpression can inhibit tumor cell proliferation and invasion [21]. Our results and other studies indicate that RGR may regulate the proliferation and invasion of glioma cells through functional interaction with CDHR1. Interestingly, the gene position between RGR and CDHR1 was close to each other on the chromosome. And a point variant of RGR with a cis-acting frameshift mutation in CDHR1 has been reported in association with recessive retinal disorder [17, 46]. Therefore, it is reasonable to speculate that RGR and CDHR1 might form a functional complex to affect glioma tumorigenesis and progression. Therefore, the protein-protein interactions between RGR and CDHR1 were performed by molecular docking. Notably, the binding site of ASP86 in RGR with the ARG378 residue of CDHR1 is able to interact to form a physical complex to regulate the proliferation and invasion of glioma cells. These results suggest that RGR and its coexpressed gene of CDHR1 are involved in cell adhesion in LGG carcinogenesis, leading to a poor prognosis in LGG patients. This study presented here expands our understanding of RGR functions and its novel roles in human cancer. However, additional work was required to evaluate the specific molecular mechanism of RGR as a tumor-negative gene in LGG, especially for the relationship among RGR, CDHR1, and retinoids. Previous studies demonstrated that retinoids strongly inhibit primary glioma cells' proliferation and migration, providing a basis for retinoids for the treatment of human malignant gliomas [47]. We also observed that the dysfunctional RGR contributes to carcinogenesis and progression in SCC by regulating the balance between cell proliferation and differentiation (unpublished data). On the basis of these promising findings, it is well worth further investigation for the relationship among RGR, CDHR1, and retinoids. Taken together, our results provide new insight into the function

of RGR in human cancer which may become a molecular target for the clinical treatment of LGG.

In conclusion, we demonstrated that the downexpression of RGR was associated with clinicopathological characteristic variables and a poor prognosis in LGG. And its molecular function was closely associated with cancer cell adhesion and adhesion molecule CDHR1. Our study revealed the potential role of RGR in tumor cell adhesion and its prognostic value, suggesting that RGR might be a prognostic biomarker or molecular target for the clinical treatment of LGG.

Supplementary information is available in the online version of the paper.

References

[1] TERAKITA A. The opsins. Genome Biol 2005; 6: 213. https://doi.org/10.1186/gb-2005-6-3-213

[2] PANDEY S, BLANKS JC, SPEE C, JIANG M, FONG HK. Cytoplasmic retinal localization of an evolutionary homolog of the visual pigments. Exp Eye Res 1994; 58: 605–613. https://doi.org/10.1006/exer.1994.1055

[3] HAO W, FONG HK. The endogenous chromophore of retinal G protein-coupled receptor opsin from the pigment epithelium. J Biol Chem 1999; 274: 6085–6090. https://doi.org/10.1074/jbc.274.10.6085

[4] MORSHEDIAN A, KAYLOR JJ, NG SY, TSAN A, FREDERIKSEN R et al. Light-Driven Regeneration of Cone Visual Pigments through a Mechanism Involving RGR Opsin in Müller Glial Cells. Neuron 2019; 102. https://doi.org/10.1016/j.neuron.2019.04.004

[5] ZHANG J, CHOI EH, TWORAK A, SALOM D, LEINONEN H et al. Photic generation of 11-retinal in bovine retinal pigment epithelium. J Biol Chem 2019; 294: 19137–19154. https://doi.org/10.1074/jbc.RA119.011169

[6] WENZEL A, OBERHUASER V, PUGH EN, LAMB TD, GRIMM C et al. The retinal G protein-coupled receptor (RGR) enhances isomerohydrolase activity independent of light. J Biol Chem 2005; 280: 29874–29884. https://doi.org/10.1074/jbc.M503603200

[7] RADU RA, HU J, PENG J, BOK D, MATA NL et al. Retinal pigment epithelium-retinal G protein receptor-opsin mediates light-dependent translocation of all-trans-retinyl esters for synthesis of visual chromophore in retinal pigment epithelial cells. J Biol Chem 2008; 283: 19730–19738. https://doi.org/10.1074/jbc.M801288200

[8] VAN HOOSER JP, ALEMAN TS, HE YG, CIDECIYAN AV, KUKSA V et al. Rapid restoration of visual pigment and function with oral retinoid in a mouse model of childhood blindness. Proc Natl Acad Sci U S A 2000; 97: 8623–8628. https://doi.org/10.1073/pnas.150236297

[9] VAN HOOSER JP, LIANG Y, MAEDA T, KUKSA V, JANG GF et al. Recovery of visual functions in a mouse model of Leber congenital amaurosis. J Biol Chem 2002; 277: 19173–19182. https://doi.org/10.1074/jbc.M112384200

[10] CHOI EH, DARUWALLA A, SUH S, LEINONEN H, PALCZEWSKI K. Retinoids in the visual cycle: role of the retinal G protein-coupled receptor. J Lipid Res 2021; 62: 100040. https://doi.org/10.1194/jlr.TR120000850

[11] TERKITA A, YAMASHITA T, SHICHIDA Y. Highly conserved glutamic acid in the extracellular IV-V loop in rhodopsins acts as the counterion in retinochrome, a member of the rhodopsin family. Proc Natl Acad Sci U S A 2000; 97: 14263–14267. https://doi.org/10.1073/pnas.260349597

[12] PARISOTTO M, BRODEUR H, BHATT PV, MADER S. [Retinoid metabolism and cancer]. Med Sci (Paris) 2006; 22: 1101–1106. https://doi.org/10.1051/medsci/200622121101

[13] TANG XH, GUDAS LJ. Retinoids, retinoic acid receptors, and cancer. Annu Rev Pathol 2011; 6: 345–364. https://doi.org/10.1146/annurev-pathol-011110-130303

[14] SHEN D, JIANG M, HAO W, TAO L, SALAZAR M et al. A human opsin-related gene that encodes a retinaldehyde-binding protein. Biochemistry 1994; 33: 13117–13125. https://doi.org/10.1021/bi00248a022

[15] CHEN XN, KORENBERG JR, JIANG M, SHEN D, FONG HK. Localization of the human RGR opsin gene to chromosome 10q23. Hum Genet 1996; 97: 720–722. https://doi.org/10.1007/BF02346179

[16] MORIMURA H, SAINDELLE-RIBEAUDEAU F, BERSON EL, DRYJA TP. Mutations in RGR, encoding a light-sensitive opsin homologue, in patients with retinitis pigmentosa. Nat Genet 1999; 23: 393–394. https://doi.org/10.1038/70496

[17] ARNO G, HULL S, CARSS K, DEV-BORMAN A, CHAKAROVA C et al. Reevaluation of the Retinal Dystrophy Due to Recessive Alleles of RGR With the Discovery of a Cis-Acting Mutation in CDHR1. Invest Ophthalmol Vis Sci 2016; 57: 4806–4813. https://doi.org/10.1167/iovs.16-19687

[18] BA-ABBAD R, LEYS M, WANG X, CHAKAROVA C, WASEEM N et al. Clinical Features of a Retinopathy Associated With a Dominant Allele of the RGR Gene. Invest Ophthalmol Vis Sci 2018; 59: 4812–4820. https://doi.org/10.1167/iovs.18-25061

[19] BAO X, ZHANG Z, GUO Y, BUSER C, KOCHOUNIAN H et al. Human RGR Gene and Associated Features of Age-Related Macular Degeneration in Models of Retina-Choriocapillaris Atrophy. Am J Pathol 2021; 191: 1454–1473. https://doi.org/10.1016/j.ajpath.2021.05.003

[20] MERMEKLIEVA E, KAMENAROVA K, MIHOVA K, SHAKOLA F, KANEVA R. A rare case of RGR/CDHR1 haplotype identified in Bulgarian patient with cone-rod dystrophy. Ophthalmic Genet 2021: 1–6. https://doi.org/10.1080/13816810.2021.1946700

[21] WANG H, WANG X, XU L, LIN Y, ZHANG J et al. Low expression of CDHR1 is an independent unfavorable prognostic factor in glioma. J Cancer 2021; 12: 5193–5205. https://doi.org/10.7150/jca

[22] GU Y, WANG Y, LAN Y, FENG J, ZENG W et al. Expression of Retinal G Protein-Coupled Receptor, a Member `of the Opsin Family, in Human Skin Cells and Its Mediation of the Cellular Functions of Keratinocytes. Front Cell Dev Biol 2022; 10: 787730. https://doi.org/10.3389/fcell.2022.787730

[23] GAO J, AKSOY BA, DOGRUSOZ U, DRESDNER G, GROSS B et al. Integrative analysis of complex cancer genomics and clinical profiles using the cBioPortal. Sci Signal 2013; 6: pl1. https://doi.org/10.1126/scisignal.2004088

[24] TANG Z, KANG B, LI C, CHEN T, ZHANG Z. GEPIA2: an enhanced web server for large-scale expression profiling and interactive analysis. Nucleic Acids Res 2019; 47: W556–W560. https://doi.org/10.1093/nar/gkz430

[25] ZHOU T, CAI Z, MA N, XIE W, GAO C et al. A Novel Ten-Gene Signature Predicting Prognosis in Hepatocellular Carcinoma. Front Cell Dev Biol 2020; 8: 629. https://doi.org/10.3389/fcell.2020.00629

[26] AN Y, WANG Q, ZHANG L, SUN F, ZHANG G et al. OS-lgg: An Online Prognostic Biomarker Analysis Tool for Low-Grade Glioma. Front Oncol 2020; 10: 1097. https://doi.org/10.3389/fonc.2020.01097

[27] VASAIKAR SV, STRAUB P, WANG J, ZHANG B. LinkedOmics: analyzing multi-omics data within and across 32 cancer types. Nucleic Acids Res 2018; 46: D956–D963. https://doi.org/10.1093/nar/gkx1090

[28] ZENG W, ZHANG W, FENG J, HE X, LU H. Expression of OPN3 in acral lentiginous melanoma and its associated with clinicohistopathologic features and prognosis. Immun Inflamm Dis 2021; 9: 840–850. https://doi.org/10.1002/iid3.438

[29] FITZGIBBONS PL, DILLON DA, ALSABEH R, BERMAN MA, HAYES DF et al. Template for reporting results of biomarker testing of specimens from patients with carcinoma of the breast. Arch Pathol Lab Med 2014; 138: 595–601. https://doi.org/10.5858/arpa.2013-0566-CP

[30] STACK EC, WANG C, ROMAN KA, HOYT CC. Multiplexed immunohistochemistry, imaging, and quantitation: a review, with an assessment of Tyramide signal amplification, multispectral imaging and multiplex analysis. Methods 2014; 70: 46–58. https://doi.org/10.1016/j.ymeth.2014.08.016

[31] BLENMAN KRM, BOSENBERG MW. Immune Cell and Cell Cluster Phenotyping, Quantitation, and Visualization Using In Silico Multiplexed Images and Tissue Cytometry. Cytometry A 2019; 95: 399–410. https://doi.org/10.1002/cyto.a.23668

[32] KRIENEN FM, GOLDMAN M, ZHANG Q, DEL ROSARIO RCH, FLORIO M et al. Innovations present in the primate interneuron repertoire. Nature 2020; 586: 262–269. https://doi.org/10.1038/s41586-020-2781-z

[33] WANG Y, LAN Y, LU H. Opsin3 Downregulation Induces Apoptosis of Human Epidermal Melanocytes via Mitochondrial Pathway. Photochem Photobiol 2020; 96: 83–93. https://doi.org/10.1111/php.13178

[34] ROBINSON DR, WU YM, LONIGRO RJ, VATS P, COBAIN E et al. Integrative clinical genomics of metastatic cancer. Nature 2017; 548: 297–303. https://doi.org/10.1016/j.cell.2015.05.001

[35] MIAO D, MARGOLIS CA, VOKES NI, LIU D, TAYLOR-WEINER A et al. Genomic correlates of response to immune checkpoint blockade in microsatellite-stable solid tumors. Nat Genet 2018; 50: 1271–1281. https://doi.org/10.1038/s41588-018-0200-2

[36] PIERCE BG, WIEHE K, HWANG H, KIM BH, VREVEN T et al. ZDOCK server: interactive docking prediction of protein-protein complexes and symmetric multimers. Bioinformatics 2014; 30: 1771–1773. https://doi.org/10.1093/bioinformatics/btu097

[37] MONGAN NP, GUDAS LJ. Diverse actions of retinoid receptors in cancer prevention and treatment. Differentiation 2007; 75: 853–870. https://doi.org/10.1111/j.1432-0436.2007.00206.x

[38] KIM H, LAPOINTE J, KAYGUSUZ G, ONG DE, LI C et al. The retinoic acid synthesis gene ALDH1a2 is a candidate tumor suppressor in prostate cancer. Cancer Research 2005; 65: 8118–8124. https://doi.org/10.1158/0008-5472

[39] MIRA-Y-LOPEZ R, ZHENG WL, KUPPUMBATTI YS, REX-ER B, JING Y et al. Retinol conversion to retinoic acid is impaired in breast cancer cell lines relative to normal cells. J Cell Physiol 2000; 185: 302–309. https://doi.org/10.1002/1097-4652(200011)185:2<302::AID-JCP15>3.0.CO;2-#

[40] ECKEL-PASSOW JE, LACHANCE DH, MOLINARO AM, DECKER PA, SICOTTE H et al. Glioma Groups Based on 1p/19q, IDH, and TERT Promoter Mutations in Tumors. N Engl J Med 2015; 372: 2499–2508. https://doi.org/10.1056/NEJMoa1407279

[41] QI ST, YU L, GUY S, DING YQ, HAN HX et al. IDH mutations predict longer survival and response to temozolomide in secondary glioblastoma. Cancer Sci 2012; 103: 269–273. https://doi.org/10.1111/j.1349-7006.2011.02134.x

[42] KIM SY, YASUDA S, TANAKA H, YAMAGATA K, KIM H. Non-clustered protocadherin. Cell Adh Migr 2011; 5: 97–105. https://doi.org/10.4161/cam.5.2.14374

[43] VAN ROY F. Beyond E-cadherin: roles of other cadherin superfamily members in cancer. Nat Rev Cancer 2014; 14: 121–134. https://doi.org/10.1038/nrc3647

[44] YU J, CHENG YY, TAO Q, CHEUNG KF, LAM CNY et al. Methylation of protocadherin 10, a novel tumor suppressor, is associated with poor prognosis in patients with gastric cancer. Gastroenterology 2009; 136: 640–51.e1. https://doi.org/10.1053/j.gastro.2008.10.050

[45] IMOTO I, IZUMI H, YOKOI S, HOSODA H, SHIBATA T et al. Frequent silencing of the candidate tumor suppressor PCDH20 by epigenetic mechanism in non-small-cell lung cancers. Cancer Res 2006; 66: 4617–4626. https://doi.org/10.1158/0008-5472.CAN-05-4437

[46] MERMEKLIEVA E, KAMENAROVA K, MIHOVA K, SHAKOLA F, KANEVA R. A rare case of RGR/CDHR1 haplotype identified in Bulgarian patient with cone-rod dystrophy. Ophthalmic Genet 2021; 42: 747–752. https://doi.org/10.1080/13816810.2021.1946700

[47] BOUTERFA H, PICHT T, KESS D, HERBOLD C, NOLL E et al. Retinoids inhibit human glioma cell proliferation and migration in primary cell cultures but not in established cell lines. Neurosurgery 2000; 46: 419–430. https://doi.org/10.1097/00006123-200002000-00029

A pan-cancer analysis of RGR opsin expression and its downregulation associated with poor prognosis in glioma

Jianglong FENG[1,2,3,#], Wei ZHANG[2,#], Wen ZENG[2,#], Yu WANG[2], Yangguang GU[2], Yinghua LAN[2], Wenxiu YANG[3], Hongguang LU[1,2,*]
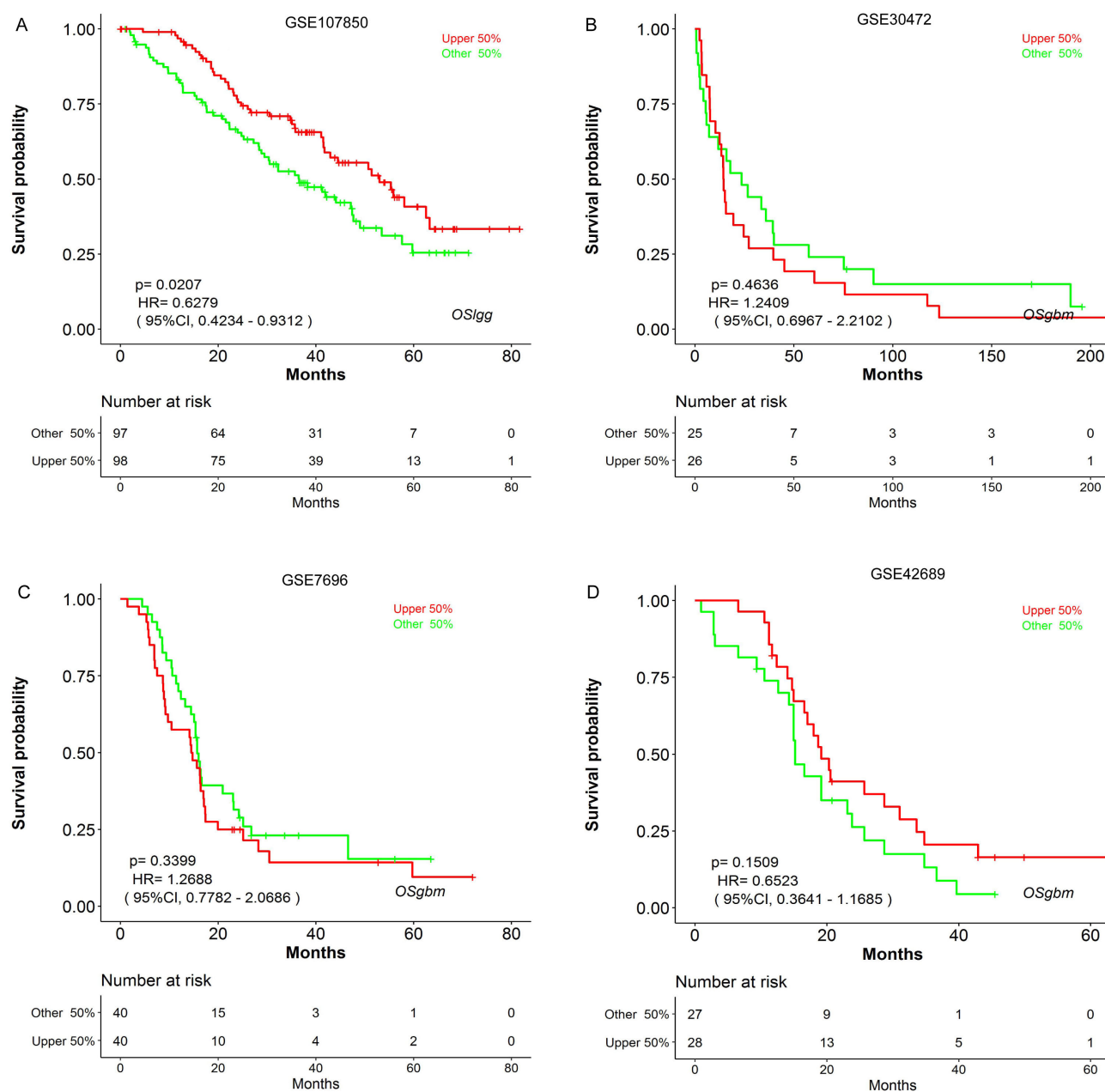
Supplementary Information
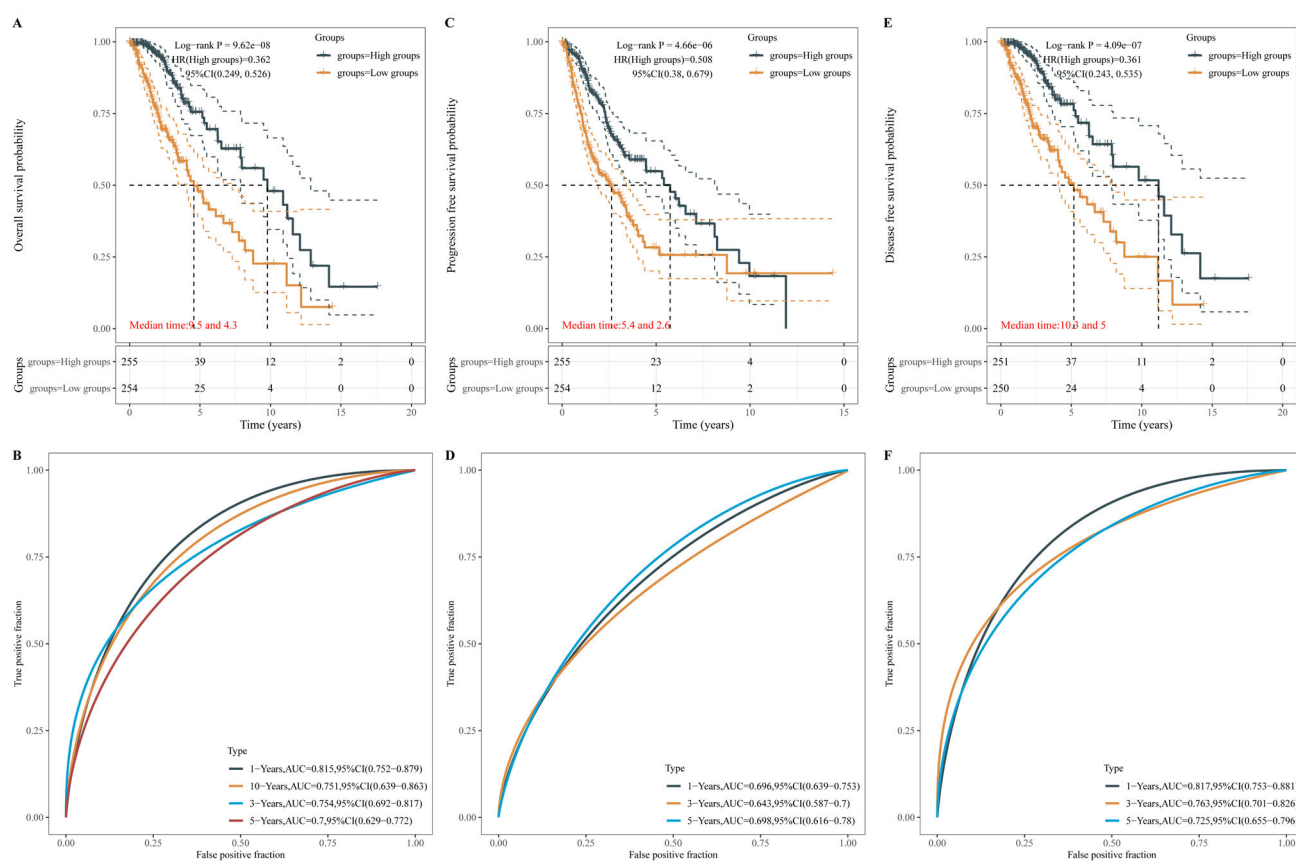
Supplementary Figure S1. Survival analysis of LGG patients between low and high expression of RGR groups according to RGR expression of median value using the Kaplan-Meier method. A) Overall survival (OS) curve of between patients with high and low expression of RGR in TCGA dataset. **B)** ROC curves showing the specificity and sensitivity of using expression levels of RGR to evaluate OS in LGG. **C)** Progression free survival (PFS) analysis of LGG patients between low and high expression of RGR groups in TCGA dataset. **D)** ROC curves showing the specificity and sensitivity of using expression levels of RGR to evaluate PFS. **E)** Disease specific survival (DSS) curve of between patients with high and low expression of RGR. **F)** ROC curves showing the specificity and sensitivity of using expression levels of RGR to evaluate DSS in TCGA dataset. RNA-sequencing expression profiles and corresponding clinical information for LGG were downloaded from the TCGA dataset (https://portal.gdc.com). Log-rank test was used to compare differences in survival between these groups. The time ROC (v 0.4) analysis was used to compare the predictive accuracy of LGG mRNA. For Kaplan-Meier curves, p-values and hazard ratio (HR) with 95% confidence interval (CI) were generated by log-rank tests and univariate cox proportional hazards regression. All the analysis methods and R packages were implemented by R (foundation for statistical computing 2020) version 4.0.3. p-value <0.05 was considered statistically significant
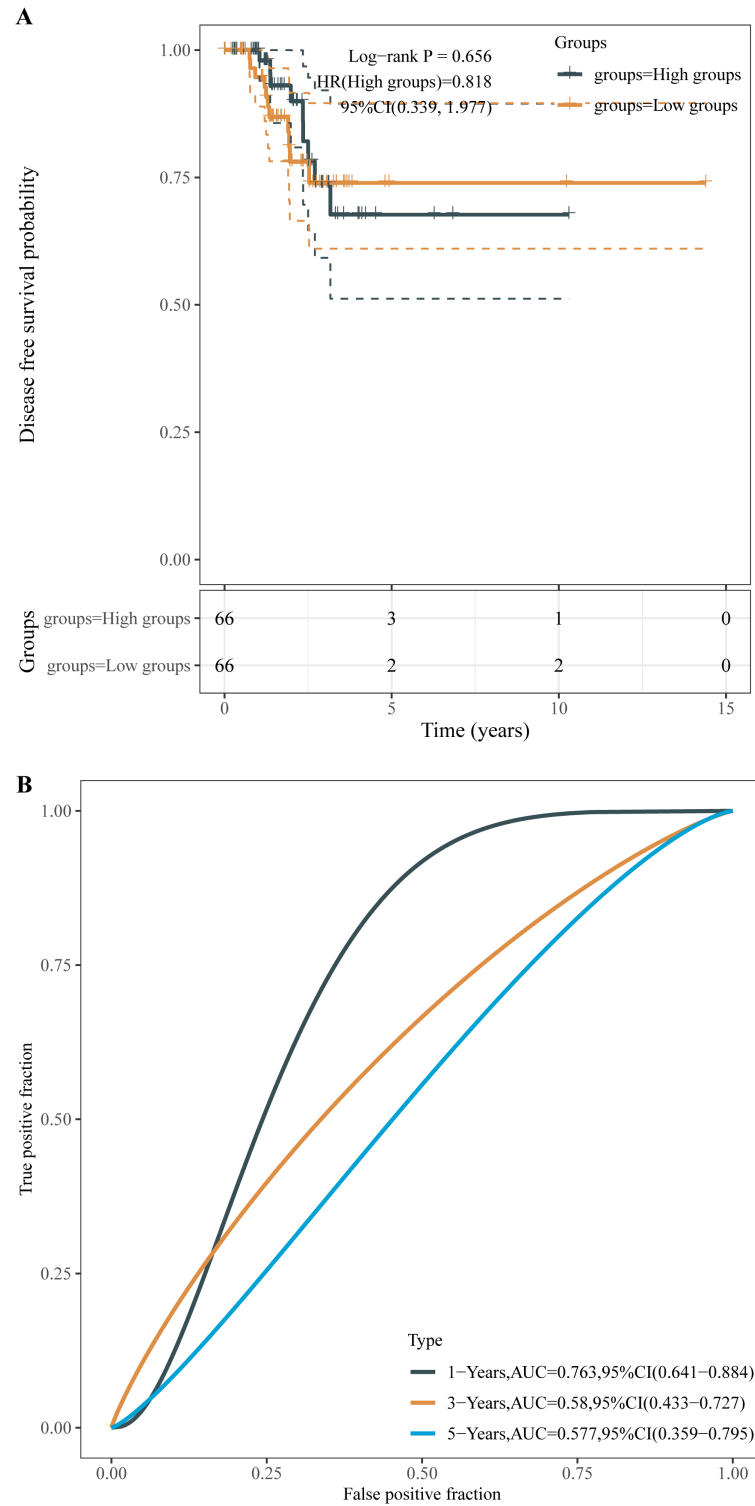
Supplementary Figure S2. Disease free survival (DFS) analysis of LGG patients between low and high expression of RGR groups in TCGA dataset. RNA-sequencing expression profiles and corresponding clinical information for LGG were downloaded from the TCGA dataset (https://portal.gdc. com). Log-rank test was used to compare differences in survival between these groups. The time ROC (v 0.4) analysis was used to compare the predictive accuracy of LGG mRNA. For Kaplan-Meier curves, p-values and hazard ratio (HR) with 95% confidence interval (CI) were generated by log-rank tests and univariate cox proportional hazards regression. All the analysis methods and R packages were implemented by R (foundation for statistical computing 2020) version 4.0.3. p-value <0.05 was considered statistically significant

Supplementary Figure S3. Survival curve of glioma patients between low and high expression of RGR groups GSE107850, GSE30472, GSE7696 and GSE42669 datasets according to RGR expression of median value using the Kaplan-Meier method.
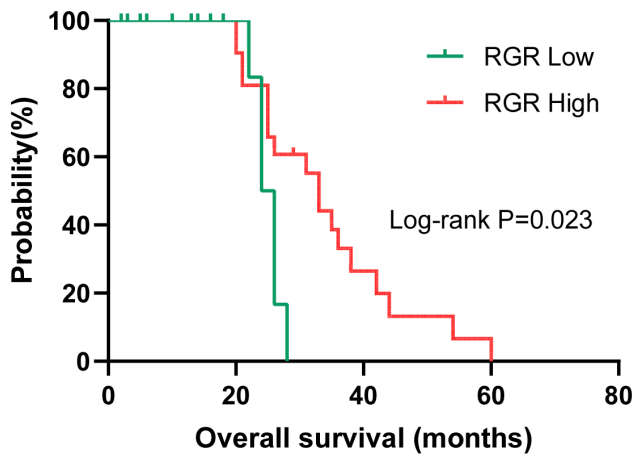
Supplementary Figure S4. Overall survival analysis of LGG patients with different IHC staining score of RGR (<120 vs.≥120).
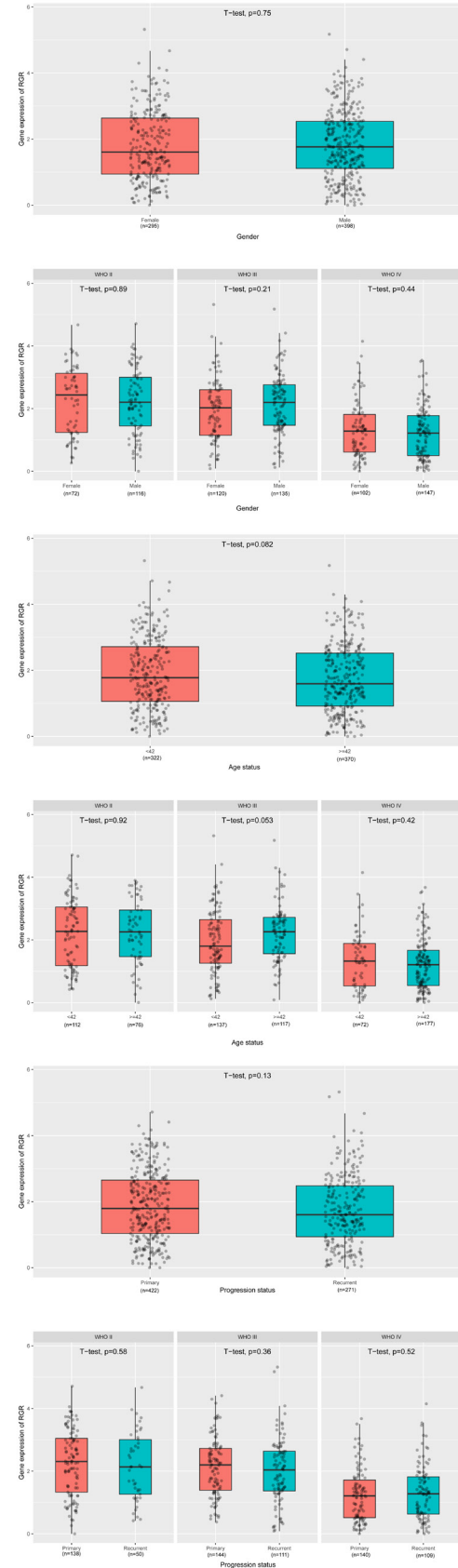
▶ **Supplementary Figure S5. Statistical comparison between RGR expression level and clinicopathological data including age, sex and progression status from CGGA dataset.**
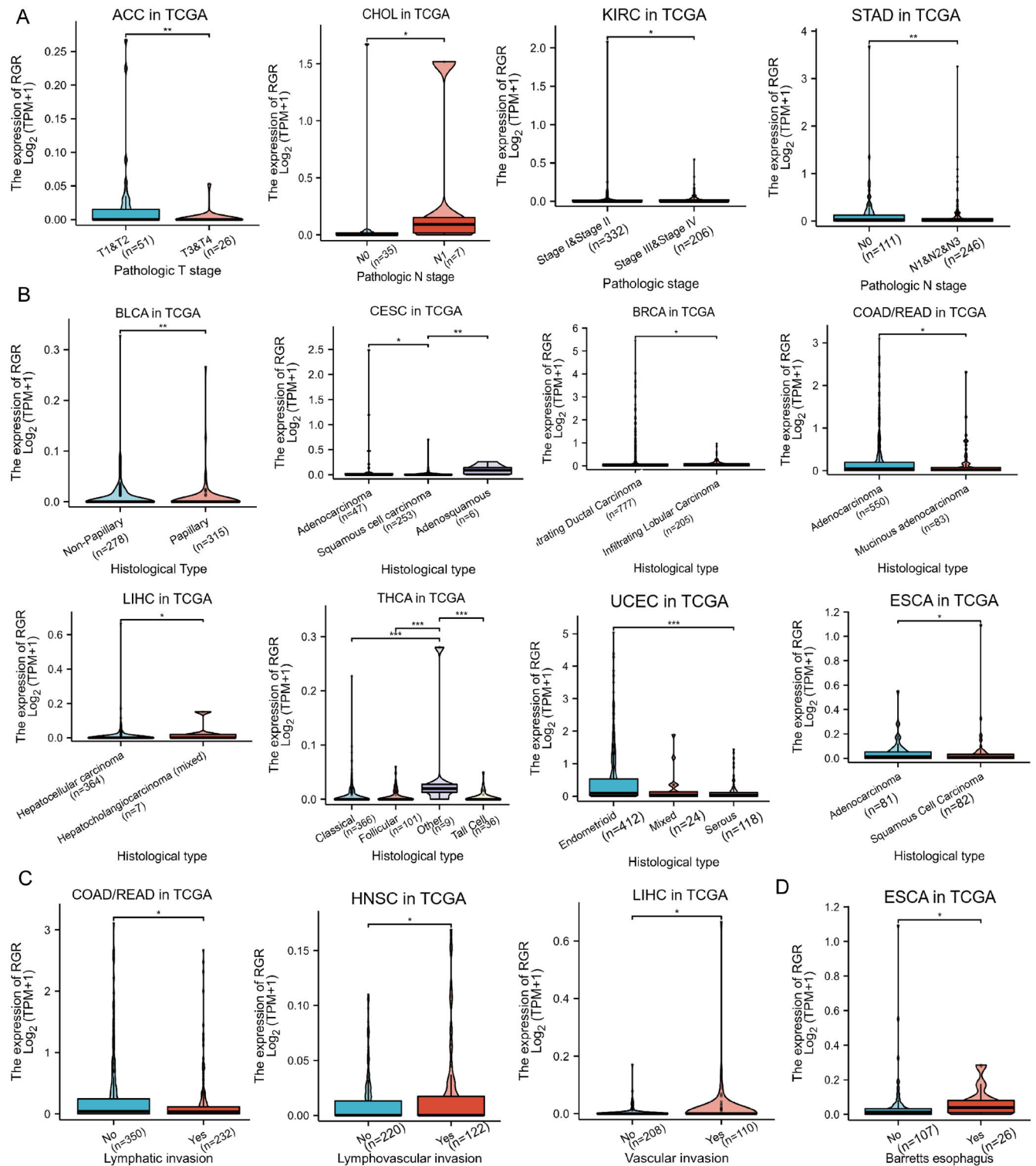
Supplementary Figure S6. Expression difference of RGR in clinical pathological stage, histological subtypes, lymphatic and vascular invasion in various cancers in TCGA dataset. A) RGR expression in pathological stage in ACC, CHOL, KIRC, STAD. B) RGR expression in histological subtypes in BLCA, CESC, BRCA, COAD/READ, LIHC, THCA, UCEC, ESCA. C) RGR expression in lymphatic and vascular invasion in COAD/READ, HNSC. D) RGR expression in Barretts esophagus medical history in ESCA.
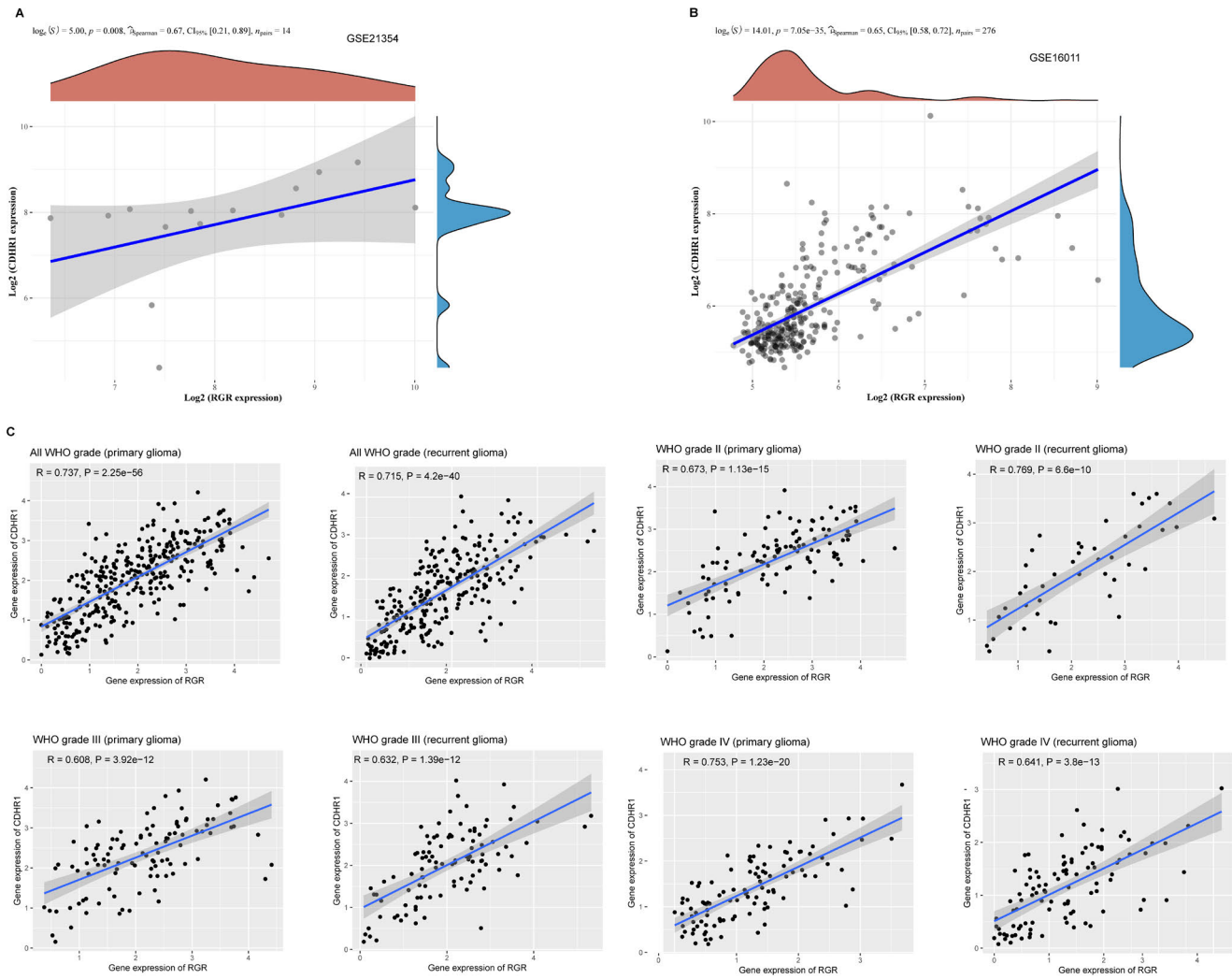
Supplementary Figure S7. Correlation analysis between RGR and CDHR1 in GSE21354 (A) and GSE16011(B) datasets and CGGA dataset (C).